Elastic/plastic semi-analytical method for arbitrary curved surfaces of scarf repaired composites

Yancheng Liu¹, Bin Liu^{1,2*}

- 1. School of Aeronautics, Northwestern Polytechnical University, Xi'an China, 710072
- 2. National Key Laboratory of Aircraft Configuration Design, Xi'an, Shaanxi 710072, P.R. China

Abstract

As scarf repair has been widely used in composite repair, analysis methods for rapid assessment of scarf joints were put forward. Basing on the modified semi-analytical method (MAM), which has restored the abrupt stress change caused by the off-axis stiffness distribution of the laminate, a semi-analytical method that is applicable to the calculation of elastic/plastic stress distribution on arbitrary curved scarf surfaces is proposed in this paper. Results derived by the extended method are basically consistent with finite element results. Additionally, the plastic strain of the adhesive is taken under consideration by introducing bilinear constitutive relation and the von Mises criteria to the adhesive. By applying the method to several examples, relations between scarf angle and stress distribution are disclosed, which would benefit the design of scarf joints.

Keywords

Semi-analytical method, Scarf joints, Scarf repair composites, Simulated annealing

1.Introduction

Though Fiber-reinforced composites have been widely used in aerospace, especially in the main bearing structure of aircrafts [1], The impact and other loads during aircraft service (such as hail impact, tool drop, sand impact, etc.) will cause latent internal damage to the composite structure, which is yet unavoidable, and needs to be repaired in time^[2]. Scarf repair has been applied to damaged composite laminates as the replacement of the whole part would cost too much, and conventional bolt repair, as Figure 1(a) shows, might cause a heavy loss of strength^[3, 4]. Scarf repair structures are often analyzed in two-dimension as Hart Smith suggested^[5].

During the past half century finite element method (FEM)^[6], analytical method^[7] and semi-analytical method^[8, 9] for the analysis of scarf joint has undergone significant development. The tendency of the research was expanding from plane scarf repair of isotropic materials to diverse geometry of scarf surfaces applied to composites^[8, 10]. In recent years, the exploration of diverse scarf surface geometries has further improved the design of scarf joint. Harman^[8] introduced average

reduction method of composite section elastic modulus, and derived a method for calculating stress distribution of two-dimensional scarf repaired composites. Additionally, they proposed an optimization method to minimize the peak shear stress of adhesive layer by optimizing the bonding angle distribution controlled by first order equation.

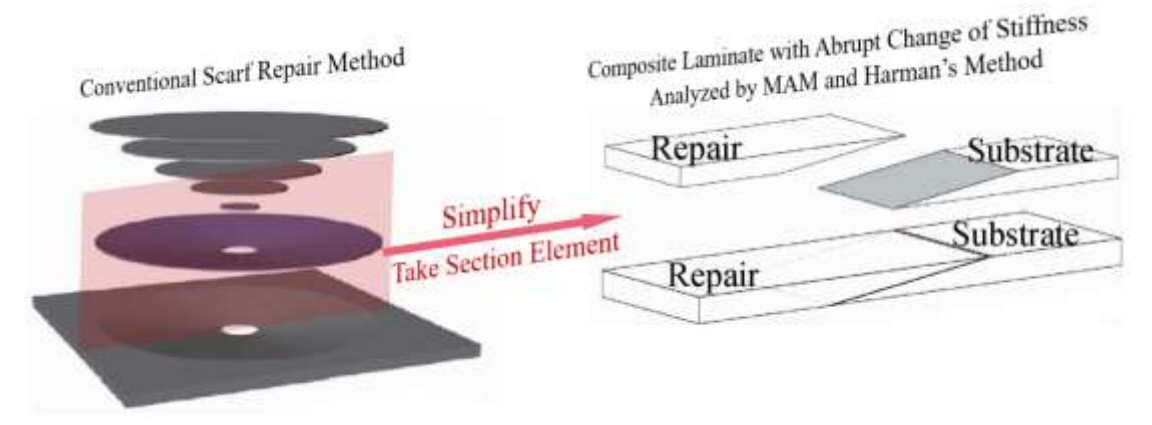


Figure 1 2D scarf joint

In spite of the convenience and versatility of FEM, extremely fine meshes around the thin adhesive could cause the surge of computation amount^[11, 12]. As for the semi-analytical method improved by Harman, the scenario is limited to certain scarf joints, and the accuracy is influenced by the through-thickness stiffness variation of composite laminates. In the analysis of scarf joint, a balance needs to be struck between the speed of analysis, the scope of application and the accuracy of results. Liu^[9] improved the method with stiffness-distribution principle and provided a modified analytical method (MAM), which has achieved a more precise and believable result in the stress distribution on plane scarf surfaces. MAM. And the application of stiffness-distribution principle has been proven concise effective by Yan^[13] with experiments.

In this paper, a semi-analytical stress distribution calculating method that is applicable to arbitrary shape surfaces of scarf repaired composites is proposed, which is achieved by setting the scarf angle as a function of thickness. The method has been proven relatively accurate by several examples in comparison with FEM. And moreover, patterns found in these examples reveal optimization criteria for following optimum design of scarf joints. To take not only the cohesive failure caused by shear stress, but also the yield of adhesive under consideration, the adhesive is regarded as elastic-plastic material. And the introduction of plastic yield implies that the damage tolerance is assignable in conventional scarf joints.

2. Stress prediction for arbitrary scarf surfaces

2.1. Model descriptions

Figure 2 illustrates a 2D scarf joint with curved scarf surface. Let the damaged laminate, the patch and the adhesive be A, B and C respectively. As the figure shows, the scarf repaired laminate is an n-ply composite laminate with a thickness of h. The load applied here is uniaxial tensile stress T_0 on the x axis, and the stress distribution to be calculated is on the adhesive with a thickness of t_c . To make the adhesive arbitrary, the adhesive in this model is considered as a curve controlled by scarf angle varies with coordinate on y.

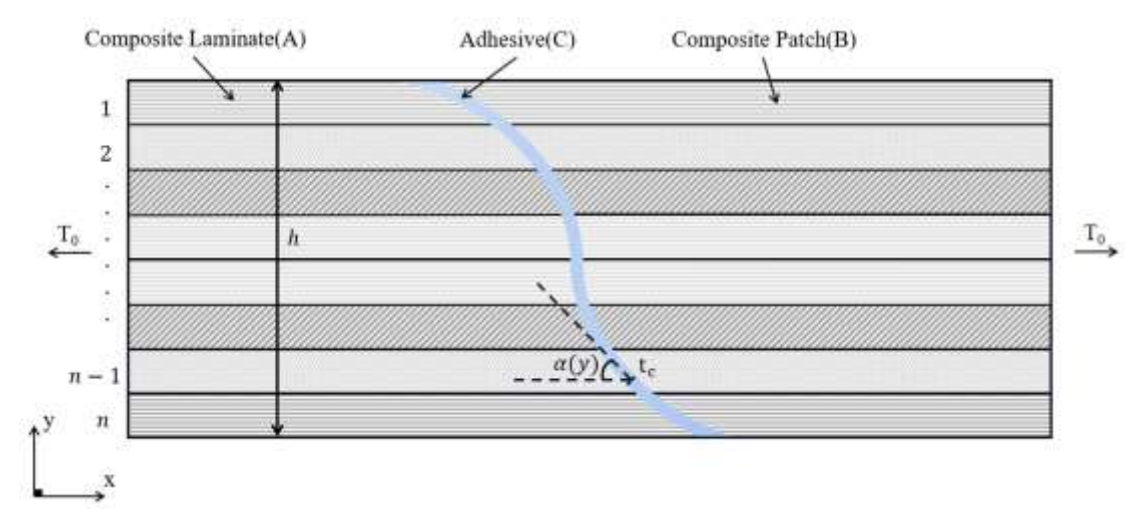


Figure 2 Scarf joint model with arbitrary scarf surface

Let σ and ε be the stress and strain of the laminate on the three axes, and the subscript index of which be the direction, that is x, y and z. Before the derivation, the basic assumption of 2D model should be made. The plate theory assumes that: no strain occurs on the z-axis, stress on the y-axis could be ignored, and strain on the y-axis is determined by Poisson effect. The assumption is summarized as,

$$\varepsilon_z = 0$$
 (1)

$$\varepsilon_{\nu} \neq 0$$
 (2)

$$\sigma_{y} = 0 \tag{3}$$

Additionally, the constant scarf angle α is replaced by function $\alpha(y)$, which depicts an arbitrary shaped scarf surface and provides an easily controlled argument for optimum design.

2.2. Stress analysis of the joint

The whole method was built on the basis of strain compatibility on the x-axis between the laminate, the adhesive and the patch. In order to get strains, the stress should be reached first. By decomposing the stress on the adhesive to normal stress $\sigma(y)$ and shear stress $\tau(y)$, equations below

are derived:

$$\sigma(y)\cos\alpha(y) = \tau(y)\sin\alpha(y) \tag{4}$$

$$\sigma(y)\sin\alpha(y) + \tau(y)\cos\alpha(y) = \sigma_T(y) \tag{5}$$

Where $\sigma_T(y)$ represents the component of stress on the adhesive on the x-axis. By integrating $\sigma_T(y)$, the load on the adhesive along the y-axis T(y) could be obtained,

$$T(y) = \int_0^y \frac{\tau(y)dy}{\sin\alpha(y)\cos\alpha(y)} \tag{6}$$

As Liu's idea is followed to acquire higher accuracy, stiffness distribution is introduced, which requires calculating stress distributions of A and B when assuming that strains on the section are the same, as Figure 3 shows. Let $E_{xA}(y)$ and $E_{xB}(y)$ be stiffness distributions of A and B along y-axis, stress distributions $\sigma_{xA}(y)$ and $\sigma_{xB}(y)$ could be expressed as,

$$\sigma_{xA}(y) = \frac{T_{xA}(y)}{dy} K_A(y) \tag{7}$$

$$\sigma_{xB}(y) = \frac{T_0 - T_{xA}(y)}{dy} K_B(y)$$
(8)

Where $T_{xA}(y)$ represents the load on the whole section of A, and $T_{xB}(y)$ is equal to $T_0 - T_{xA}(y)$, specifically

$$T_{xA}(y) = \int_0^y \frac{\tau(y)dy}{\sin\alpha(y)\cos\alpha(y)} \tag{9}$$

 $K_A(y)$ and $K_B(y)$ represents contribution factors in stiffness contribution theory, which are

$$K_{A}(y) = \frac{\int_{y}^{y+dy} E_{xA}(y)dy}{\int_{y}^{h} E_{xA}(y)dy}$$
(10)

$$K_B(y) = \frac{\int_{y-dy}^{y} E_{xB}(y) dy}{\int_{0}^{y} E_{xB}(y) dy}$$
(11)

2.3. Strain compatibility equation

The elementary strain compatibility equation in scarf joint is

$$\varepsilon_{xA}(y) - \varepsilon_{xB}(y) = \varepsilon_{xc}(y)$$
 (12)

 $\varepsilon_{xA}(y)$, $\varepsilon_{xB}(y)$ and $\varepsilon_{xc}(y)$ are strains of A, B and C on the same y coordination. According to generalized Hooke's law and plate theory assumptions above,

$$\varepsilon_{x} = \frac{\sigma_{x}}{E_{x}} (1 - \mu_{xz} \mu_{zx}) \tag{13}$$

For $\sigma_{xA}(y)$ and $\sigma_{xB}(y)$ have been derived above, by substituting them into Eq.(13), we find strains of A and B adjoining the adhesive,

$$\varepsilon_{xA}(y) = \frac{T_A(y)K_A(y)}{E_{xA}(y)dy} \left(1 - \mu_{xzA}(y)\mu_{zxA}(y)\right) \tag{14}$$

$$\varepsilon_{xB}(y) = \frac{(T_0 - T_A(y))K_B(y)}{E_{xB}(y)dy} (1 - \mu_{xzB}(y)\mu_{zxB}(y))$$
 (15)

As $\sigma_{xA}(y)$ and $\sigma_{xB}(y)$ change along the adhesive, $\varepsilon_{xA}(y)$ and $\varepsilon_{xB}(y)$ actually represent rates of displacement along the adhesive.

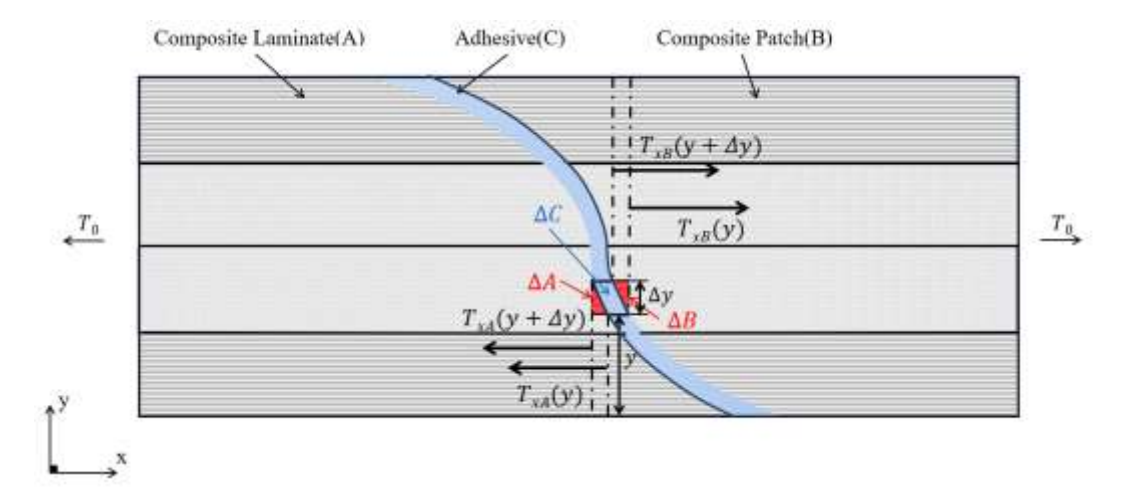


Figure 3 Elements for stiffness distribution

According to the physical significance of $\varepsilon_{xc}(y)$, which is the displacement rate of C. It's noteworthy that $\varepsilon_{xc}(y)$ should be derived with respect to x for displacement on the x-axis are $\varepsilon_{xA}(y)dx$ and $\varepsilon_{xB}(y)dx$. The displacement $\Delta u_{xc}(y)$ could be simplified by relation between $\sigma(y)$ and $\tau(y)$, which is,

$$\Delta u_{xc}(y) = \frac{\sigma(y)}{E_c} t_c sin\alpha(y) + \frac{\tau(y)}{G_c} t_c cos\alpha(y) = \left[\frac{sin^2\alpha(y)}{cos\alpha(y)E_c} + \frac{cos\alpha(y)}{G_c} \right] \tau(y) t_c \tag{16}$$

Since $\frac{\delta y}{\delta x} = tan\alpha(y)$, by differentiating Eq. (16),

$$\varepsilon_{xc}(y) = \frac{\delta \Delta u_{xc}(y)}{\delta x} = \frac{\delta \Delta u_{xc}(y)}{\delta y} \frac{\delta y}{\delta x}$$

$$= \left(\frac{2\sin^2 \alpha(y)\cos^2 \alpha(y) + \sin^4 \alpha(y)}{\cos^3 \alpha(y)E_c} - \frac{\sin^2 \alpha(y)}{\cos \alpha(y)G_c}\right) \alpha'(y)\tau(y)t_c + \left(\frac{\sin^3 \alpha(y)}{\cos^2 \alpha(y)E_c} + \frac{\sin \alpha(y)}{G_c}\right)\tau'(y)t_c (17)$$

As $\varepsilon_{xA}(y)$, $\varepsilon_{xB}(y)$ and $\varepsilon_{xc}(y)$ are derived, according to Eq. (12), the governing equation of $\tau(y)$ is,

In order to adapt the equation to known boundary condition T(y), relations between $\tau(y)$, $\tau'(y)$ and T'(y), T''(y) are built. By differentiating Eq. (9),

$$T'(y) = \frac{\tau(y)}{\sin\alpha(y)\cos\alpha(y)} \tag{19}$$

$$T''(y) = \frac{\tau'(y)}{\sin\alpha(y)\cos\alpha(y)} + (\frac{1}{\cos^2\alpha(y)} - \frac{1}{\sin^2\alpha(y)})\alpha'(y)\tau(y)$$
(20)

Thus, $\tau(y)$ and $\tau'(y)$ are,

$$\tau(y) = \sin\alpha(y)\cos\alpha(y)T'(y) \tag{21}$$

$$\tau'(y) = \sin\alpha(y)\cos\alpha(y)T''(y) - [\sin^2\alpha(y) - \cos^2\alpha(y)]\alpha'(y)T'(y) \tag{22}$$

After replacing T'(y) and T''(y) in Eq. (18) by $\tau(y)$ and $\tau'(y)$, the governing equation of T(y) is,

$$p(y)T''(y) + q(y)T'(y) + r(y)T(y) + g(y) = 0$$
(23)

Where

$$p(y) = \frac{t_c}{E_c G_c} \left(\frac{\sin^4 \alpha(y)}{\cos \alpha(y)} G_c + \sin^2 \alpha(y) \cos \alpha(y) E_c \right)$$

$$q(y) = \frac{t_c \alpha'(y)}{E_c G_c} (3 \sin^3 \alpha(y) G_c - 2 \sin^3 \alpha(y) E_c + \sin \alpha(y) \cos^2 \alpha(y) E_c)$$

$$r(y) = -\left(\frac{1 - \mu_{xzB}(y) \mu_{zxB}(y)}{E_{xB}(y) dy} K_B(y) + \frac{1 - \mu_{xzA}(y) \mu_{zxA}(y)}{E_{xA}(y) dy} K_A(y) \right)$$

$$g(y) = \frac{1 - \mu_{xzB}(y) \mu_{zxB}(y)}{E_{xB}(y) dy} K_B(y) T_0$$

2.4. Introduction of plastic strain

As Cheng's study indicates, repaired composite laminates don't crack all of a sudden, on the contrary, it starts in high-stress sections and gradually expands to adjoining adhesive^[14]. Therefore, under a circumstance that the adhesive is plasticized, which is usual for epoxy adhesive nowadays, the failure tolerance could be theoretically improved by distributing the peak stress to surrounding linear elastic regions^[15]. In order to restore the plasticity of the adhesive in our model, bilinear model is used to which to describe its constitutive relationship. For it being a typical isotropic elastic/plastic analysis, von Mises criterion is used to calculate where the local plastic yield would occur. Principal stresses $\sigma_1(y)$, $\sigma_2(y)$ and $\sigma_3(y)$ are:

$$\sigma_1(y) = \frac{\sigma(y)}{2} + \sqrt{\tau(y)^2 + \frac{\sigma(y)^2}{4}}$$
 (24)

$$\sigma_2(y) = 0 \tag{25}$$

$$\sigma_3(y) = \frac{\sigma(y)}{2} - \sqrt{\tau(y)^2 + \frac{\sigma(y)^2}{4}}$$
 (26)

Which leads to the von Mises stress on the adhesive σ_v ,

$$\sigma_{\nu}(y) = \sqrt{\frac{1}{2}[(\sigma_1 - \sigma_2)^2 + (\sigma_2 - \sigma_3)^2 + (\sigma_3 - \sigma_1)^2]} = \sqrt{\tan^2\alpha(y) + 3} \times \tau(y)$$
 (27)

According to the criterion, when $\sigma_v(y) \ge \sqrt{3}\tau_{plastic}$, local plastic strain occurs on the part of the adhesive, displacement equation $\Delta u_{xc}(y)$ is,

$$\Delta u_{xc}(y) = \left[\frac{\sin^2 \alpha(y)}{\cos \alpha(y) E_c} + \frac{\cos \alpha(y)}{G_c} \right] \sqrt{\frac{3}{\tan^2 \alpha(y) + 3}} \tau_{plastic} t_c$$

$$+ \left[\frac{\sin^2 \alpha(y)}{\cos \alpha(y) E_{cplas}} + \frac{\cos \alpha(y)}{G_{cplas}} \right] [\tau(y)$$

$$- \sqrt{\frac{3}{\tan^2 \alpha(y) + 3}} \tau_{plastic}] t_c$$
(28)

Differentiate $\Delta u_{xc}(y)$ as it is done above,

$$\varepsilon_{xc}(y) = \left(\frac{2\sin^{2}\alpha(y)\cos^{2}\alpha(y) + \sin^{4}\alpha(y)}{\cos^{3}\alpha(y)E_{cplas}} - \frac{\sin^{2}\alpha(y)}{\cos\alpha(y)G_{cplas}}\right)\alpha'(y)\tau(y)t_{c} \\
+ \left(\frac{\sin^{3}\alpha(y)}{\cos^{2}\alpha(y)E_{cplas}} + \frac{\sin\alpha(y)}{G_{cplas}}\right)\tau'^{(y)t_{c}} \\
+ 2\sqrt{3}\sin^{2}\alpha(y)\left(1 + 2\cos^{2}\alpha(y)\right)^{-\frac{3}{2}}\left[\left(2 + \cos^{2}\alpha(y)\right) \cdot \left(\frac{1}{E_{c}} - \frac{1}{E_{cplas}}\right)\right] \\
- (1 + \cos^{2}\alpha(y)) \cdot \left(\frac{1}{G_{c}} - \frac{1}{G_{cplas}}\right)\left[\alpha'(y)\tau_{plastic}t_{c}\right] \tag{29}$$

Considering that $\varepsilon_{xA}(y)$ and $\varepsilon_{xB}(y)$ stay the same, the governing equation of T(y) can be obtained:

$$p_{nlas}(y)T''(y) + q_{nlas}(y)T'(y) + r_{nlas}(y)T(y) + g_{nlas}(y) = 0$$
(30)

Where:

$$\begin{aligned} \mathbf{p}_{\text{plas}}(\mathbf{y}) &= \frac{t_c}{E_{cplas}} G_{cplas} \left(\frac{\sin^4 \alpha(y)}{\cos \alpha(y)} G_{cplas} + \sin^2 \alpha(y) \cos \alpha(y) E_{cplas} \right) \\ \mathbf{q}_{\text{plas}}(\mathbf{y}) &= \frac{t_c \alpha'(y)}{E_{cplas}} G_{cplas} \left(3\sin^3 \alpha(y) G_{cplas} - 2\sin^3 \alpha(y) E_{cplas} + \sin \alpha(y) \cos^2 \alpha(y) E_{cplas} \right) \\ \mathbf{r}_{\text{plas}}(\mathbf{y}) &= -(\frac{1 - \mu_{xzB}(y) \mu_{zxB}(y)}{E_{xB}(y) dy} K_B(y) + \frac{1 - \mu_{xzA}(y) \mu_{zxA}(y)}{E_{xA}(y) dy} K_A(y)) \\ \mathbf{g}_{\text{plas}}(\mathbf{y}) &= \frac{1 - \mu_{xzB}(y) \mu_{zxB}(y)}{E_{xB}(y) dy} K_B(y) T_0 + 2\sqrt{3} \sin^2 \alpha(y) (1 + 2\cos^2 \alpha(y))^{-\frac{3}{2}} [(2 + \cos^2 \alpha(y)) \cdot \left(\frac{1}{E_C} - \frac{1}{E_{xyloc}} \right) - (1 + \cos^2 \alpha(y)) \cdot \left(\frac{1}{G_C} - \frac{1}{G_{xyloc}} \right)]\alpha'(y) \tau_{plastic} t_c \end{aligned}$$

2.5. Solution of governing equations

Finite difference method is adopted to calculate the numerical solution of governing equations derived above, specifically Eq. (23) and Eq. (30). Finite difference method divides T(y) into n portions

equally, and for any node $T(y_{i+1})$ in T(y), it could be expressed as,

$$T(y_{i+1}) = \frac{[4p(y_i) - 2h^2r(y_i)]T(y_i) - 2h^2g(y_i)}{2p(y_i) + hq(y_i)} - T(y_{i-1})$$
(31)

Where h represents increment between the nodes. As for boundary conditions, they are obviously T(0) = 0 and $T(h) = T_0$. The normal stress $\sigma(y)$ and shear stress $\tau(y)$ of the adhesive can be obtained by the deformation of Eqs. (4) and (6) respectively, that is,

$$\tau(y) = T'(y)\sin\alpha(y)\cos\alpha(y) \tag{32}$$

$$\sigma(y) = T'(y)\sin^2\alpha(y) \tag{33}$$

3. Examples and results of several scarf joints

3.1. Parameters of the model

Though models chosen here vary in layups and geometries of scarf surfaces, most of their mechanical properties and basic geometries are the same. For the laminate, set the thickness h = 3mm, for the adhesive, set the thickness t = 0.2mm. The mechanical properties of both the laminate and the adhesive, which refer to IM7/977-33 CFRP and FM73 film adhesive^[16], are shown in Table 1. A constant axial load of $T_0 = 1200N$ is applied to the model.

Composite laminate Properties Adhesive Young's modulus (GPa) 162 1.15 Transverse modulus (GPa) 16.2 Shear modulus (GPa) 7.2 0.4423 Longitudinal Poisson's ratio 0.3 0.3 0.03 Transverse Poisson's ratio

Table 1 Mechanical properties of the laminate and the adhesive

3.2. FEM and semi-analytical method in plane scarf scenario

Firstly, the reliability of the method is preliminary verified by comparing the analysis results of 5° flat scarf joint processed by FEM, Harman's method and the modified method. Examples used in this section are from^[9], in which the layup is: $[45/-45/90/0/0/045/0/0/-45/90]_s$. And the output is the shear stress $\tau(y)$ on the middle of the adhesive, which is the worthiest data indicating adhesive failure. The ratio of local shear stress $\tau(y)$ to the average shear stress τ_{av} on the adhesive is introduced to represent the distribution of shear stress, where,

$$\tau_{av} = \frac{T_0}{h} \sin\alpha \cos\alpha \tag{34}$$

Figure 4 shows shear stress distribution on the adhesive. Table 2 shows Harman's, the modified

method and FEM results and the relative errors respectively. In this example, the modified method shows better accuracy in local peak values and low stress regions than Harman's method. Moreover, the trend is basically in line with the FEM result, which reflects the stiffness of the laminate, and the error is within the acceptable range.

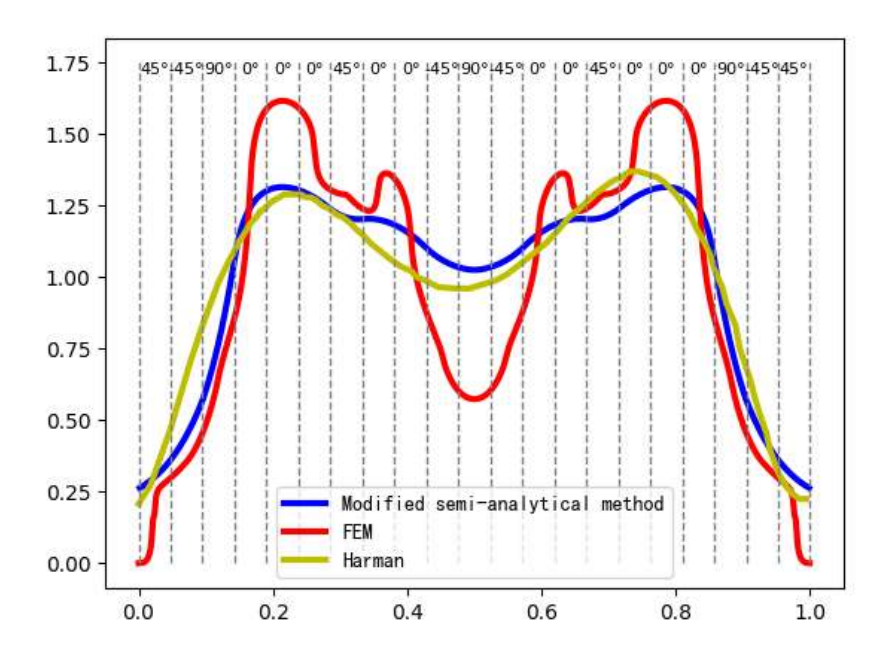


Figure 4 The shear stress distribution of 21-ply example calculated by modified semi-analytical method, FEM and Harman's method

Table 2 The shear stress distribution and relative errors of 21-ply example

Ply Angle/(°)	Sequence	FEM	modified semi- analytical method	modified semi- analytical method Error/%	Harman	Harman Error/%
45	1	0.20	0.30	53.7	0.31	57.1
-45	2	0.36	0.45	26.1	0.66	83.5
90	3	0.66	0.78	18.9	0.98	49.0
0	4	1.37	1.25	-8.4	1.19	-13.2
0	5	1.62	1.32	-18.7	1.29	-20.5
0	6	1.42	1.28	-10.4	1.27	-10.4
45	7	1.29	1.21	-6.1	1.20	-7.0
0	8	1.32	1.20	-9.1	1.10	-16.8

0	9	1.14	1.15	0.8	1.02	-10.3
-45	10	0.72	1.06	47.8	0.96	34.0
90	11	0.57	1.03	78.8	0.97	69.6

3.3. Semi-analytical method for arbitrary scarf surfaces

Several geometries of scarf surfaces are analyzed by the method, and some patterns between the scarf surface and shear stress distribution have been found. To make a concise and clear example, the layup is specified as [45/0/-45/90]2s. Two constant scarf angles of 3° and 5° are selected, other angle distributions make dimensions occupied on the x-axis be the same as 3° or 5° plane scarf repair. Figure 5 shows the distribution of scarf angles adopted here versus y-axis. The angle distributions are quadratic functions of y, for the average scarf angle of 5°, the functions are,

$$\alpha(y) = -y^2 + 3y + 3.6$$

$$\alpha(y) = -2y^2 + 6y + 2.42$$

For the average scarf angle of 3°,

$$\alpha(y) = -y^2 + 3y + 1.67$$

Shear stress distributions caused by different scarf angle distributions are illustrated in Figure 6. The most notable difference is caused by average scarf angle, as it decreases, the overall level of shear stress is significantly reduced. The reason leading to appearance above is that a smaller scarf angle provides a larger scarf surface to share load, which has been uncovered by several researches^[17, 18]. For the relation between local shear stress and scarf angle, at a certain average scarf angle, it can be seen that the shear stress drops where the scarf angle decreases, and vice versa. In this example, peak shear stresses are controlled by scarf angle. However, the stress would not disappear, but merely be redistributed to other regions where scarf angle increases. This conclusion proves that it is a feasible optimization idea to control the shear stress distribution by a more complex scarf angle distribution equation, so as to average the stress distribution and minimize the peak value.

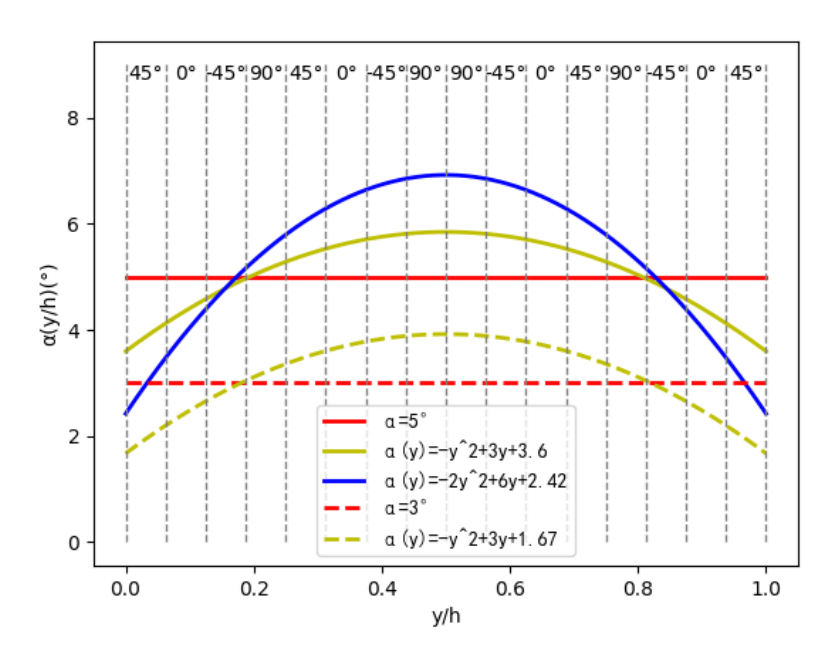


Figure 5 Preset scarf angle distribution

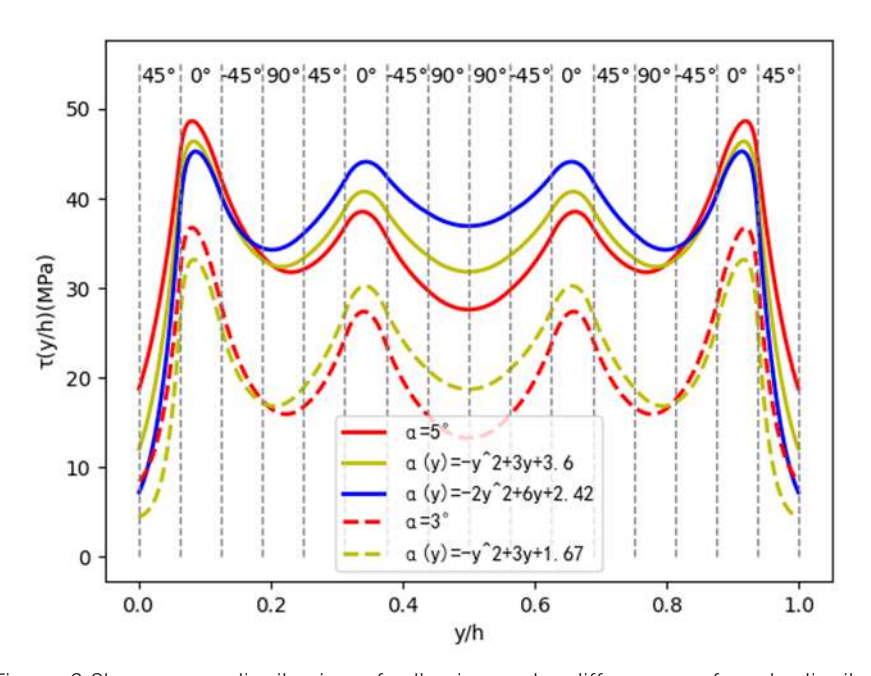


Figure 6 Shear stress distribution of adhesive under different scarf angle distribution

3.4. Examples introducing local plastic yield

The mechanical properties and loading methods used are the same, layup selected here is still [45/0/-45/90]2s. A bilinear elastic/plastic constitutive model is introduced to the adhesive, the elastic part remains the same. And after the elastic limit, the stiffness of the plastic part is 1/10 of the elastic part. The distribution of shear stress $\tau(y)$ and von Mises stress $\sigma_v(y)$ is shown in Figure 7, the dotted line version of the distributions are results of elastic scenario, and the elastic limit of von Mises stress is

marked as yellow dotted line.

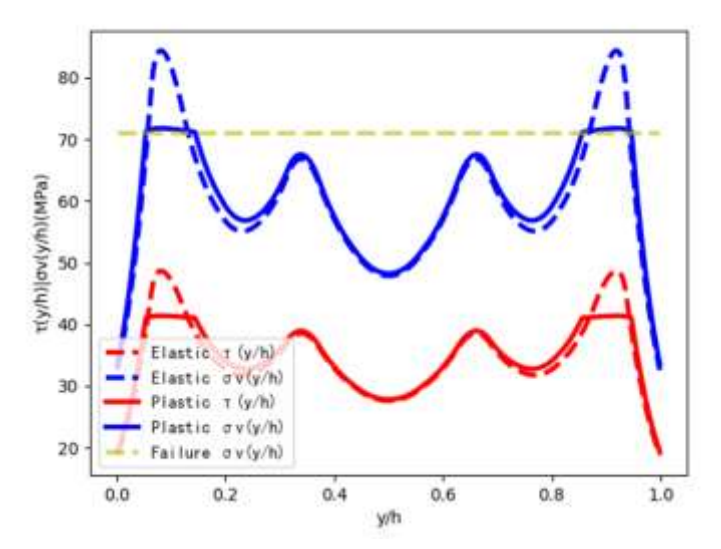


Figure 7 Distributions of von Mises stress and shear stress before and after the introduction of local plastic yield in 16-ply laminate

It can be seen that the introduction of local plastic yield makes the portion of von Mises stress above the elastic limit reduce due to a significant reduction in stiffness, which caused the peak stress be distributed to elastic regions nearby. Under a certain allowable stress, plastic yield is unacceptable in the routine service of scarf joints. However, patterns uncovered by the analysis indicates that the damage tolerance of conventional scarf joints is appreciable, and there's a significant potential bearing capacity waiting to be developed.

4. Conclusions

This paper proposed a semi-analytical method to provide rapid and relatively accurate analysis for scarf joint with arbitrary scarf surfaces. Stiffness distribution was introduced to restore the stress concentrations in laminates, and the influence caused by local plastic yield of the adhesive was considered. The reliability of the proposed method was verified by comparing with FEM and Harman's results in several typical examples. By constructing functions of scarf angle, patterns between scarf angle and shear stress were found, and those patterns provided enlightening thought for optimum design of scarf joints. The introduction of local plasticity indicates that the damage tolerance of scarf repair structures is relatively considerable, and the research on the bearing capacity of the plastic stage is promising.

Acknowledgement

The authors would like to thank the National Natural Science Foundation of China under Contracts (No. 52372094, 51902256) for the support in this research. The authors thank Aeronautical Science Foundation of China under Contracts (No. 2023Z009053001).

Copyright Statement

The authors confirm that they, and/or their company or organization, hold copyright on all of the original material included in this paper. The authors also confirm that they have obtained permission, from the copyright holder of any third party material included in this paper, to publish it as part of their paper. The authors confirm that they give permission, or have obtained permission from the copyright holder of this paper, for the publication and distribution of this paper as part of the ICAS proceedings or as individual off-prints from the proceedings.

References

- [1] MAGAZINE A J T B C, <u>HTTP://WWW</u>. BOEING. COM/COMMERCIAL/AEROMAGAZINE/ARTICLES/QTR_4_06/ARTICLE_04 _2. HTML. Boeing 787: From the ground up [J]. 2006.
- [2] KUMAR P, RAI B J C S. Delaminations of barely visible impact damage in CFRP laminates [J]. 1993, 23(4): 313-8.
- [3] CAMANHO P P, LAMBERT M J C S, TECHNOLOGY. A design methodology for mechanically fastened joints in laminated composite materials [J]. 2006, 66(15): 3004-20.
- [4] CAMANHO P P, MATTHEWS F J J O C M. A progressive damage model for mechanically fastened joints in composite laminates [J]. 1999, 33(24): 2248-80.
- [5] HART-SMITH L. Adhesive-bonded scarf and stepped-lap joints [R], 1973.
- [6] GUNNION A J, HERSZBERG I J C S. Parametric study of scarf joints in composite structures [J]. 2006, 75(1-4): 364-76.
- [7] LI D, QING G, LIU Y J C S. A three-dimensional semi-analytical model for the composite laminated plates with a stepped lap repair [J]. 2011, 93(7): 1673-82.
- [8] HARMAN A B, WANG C H J C S. Improved design methods for scarf repairs to highly strained composite aircraft structure [J]. 2006, 75(1-4): 132-44.
- [9] LIU B, XU F, JI Z J A M C S. Modified Semi-analytical Method for Adhesive Stress of Scarf Joints in Composite structure [J] [J]. 2015, 32(2): 526-33.
- [10] ORSATELLI J-B, PAROISSIEN E, LACHAUD F, et al. Bonded flush repairs for aerospace composite structures: A review on modelling strategies and application to repairs optimization, reliability and durability [J]. 2023, 304: 116338.
- [11] HE D, SAWA T, IWAMOTO T, et al. Stress analysis and strength evaluation of scarf adhesive joints subjected to static tensile loadings [J]. 2010, 30(6): 387-92.

- [12] HE X J I J O A, ADHESIVES. A review of finite element analysis of adhesively bonded joints [J]. 2011, 31(4): 248-64.
- [13] YAN B, TONG M, FURTADO C, et al. An Improved Semi-analytical Method for the strength prediction of composite bonded scarf repairs [J]. 2023, 306: 116537.
- [14] XIAOQUAN C, BAIG Y, RENWEI H, et al. Study of tensile failure mechanisms in scarf repaired CFRP laminates [J]. 2013, 41: 177-85.
- [15] PARDOEN T, FERRACIN T, LANDIS C, et al. Constraint effects in adhesive joint fracture [J]. 2005, 53(9): 1951-83.
- [16] CHALKLEY P D, VAN DEN BERG J. On obtaining design allowables for adhesives used in the bonded-composite repair of aircraft [M]. DSTO Aeronautical and Maritime Research Laboratory Melbourne Victoria, Australia, 1998.
- [17] ADKINS D W, PIPES R B. Tensile behavior of bonded scarf joints between composite adherends; proceedings of the Japan-US Conference on Composite Materials, F, 1989 [C].
- [18] ADIN H J I J O M S. The investigation of the effect of angle on the failure load and strength of scarf lap joints [J]. 2012, 61(1): 24-31.